NIH Public Access
Author Manuscript
Circ Heart Fail. Author manuscript; available in PMC 2015 July 01.

Published in final edited form as:
Circ Heart Fail. 2014 July ; 7(4): 619–626. doi:10.1161/CIRCHEARTFAILURE.113.001273.

A Bioengineered Hydrogel System Enables Targeted and Sustained Intramyocardial Delivery of Neuregulin, Activating the Cardiomyocyte Cell Cycle and Enhancing Ventricular Function in a Murine Model of Ischemic Cardiomyopathy

Jeffrey E. Cohen, MD[1,2], **Brendan P. Purcell, PhD**[3], **John W. MacArthur Jr, MD**[1,2], **Anbin Mu, DVM**[4], **Yasuhiro Shudo, MD**[1], **Jay B. Patel, BS**[1], **Christopher M. Brusalis, BA**[2], **Alen Trubelja, BS**[2], **Alexander S. Fairman, BA**[2], **Bryan B. Edwards, BS**[1], **Mollie S. Davis, BS**[3], **George Hung, BA**[2], **William Hiesinger, MD**[2], **Pavan Atluri, MD**[2], **Kenneth B. Margulies, MD**[4], **Jason A. Burdick, PhD**[3], and **Y. Joseph Woo, MD**[1]

[1]Stanford University, Department of Cardiothoracic Surgery, Stanford, CA

[2]Department of Surgery, Division of Cardiovascular Surgery, University of Pennsylvania, Philadelphia, PA

[3]Department of Bioengineering, University of Pennsylvania, Philadelphia, PA

[4]Department of Cardiology, University of Pennsylvania, Philadelphia, PA

Abstract

Background—Neuregulin (NRG) is a member of the epidermal growth factor family possessing a critical role in cardiomyocyte development and proliferation. Systemic administration of NRG demonstrated efficacy in cardiomyopathy animal models, leading to clinical trials employing daily NRG infusions. This approach is hindered by requiring daily infusions and off-target exposure. Therefore, this study aimed to encapsulate NRG in a hydrogel (HG) to be directly delivered to the myocardium, accomplishing sustained localized NRG delivery.

Methods and Results—NRG was encapsulated in HG and release over 14 days confirmed by ELISA in vitro. Sprague-Dawly rats were utilized for cardiomyocyte isolation. Cells were stimulated by PBS, NRG, HG, or NRG-HG and evaluated for proliferation. Cardiomyocytes demonstrated EdU and phosphorylated histone-H3 (PH3) positivity in the NRG-HG group only. For in vivo studies, 2 month old mice (n=60) underwent LAD ligation and were randomized to the 4 treatment groups mentioned. Only NRG-HG treated mice demonstrated PH3 and Ki67 positivity along with decreased caspase-3 activity compared to all controls. NRG was detected in myocardium 6 days following injection without evidence of off-target exposure in NRG-HG animals. At 2 weeks, the NRG-HG group exhibited enhanced LVEF, decreased LV area, and augmented borderzone thickness.

Correspondence to, Y. Joseph Woo, MD, Stanford University School of Medicine; Department of Cardiothoracic Surgery, Falk Building; CV 235; 300 Pasteur Drive; Stanford, CA 94305-3828, Phone: 650-725-3828 Fax: 650-497-6795, joswoo@stanford.edu.

Disclosures
None.

NIH-PA Author Manuscript
NIH-PA Author Manuscript
NIH-PA Author Manuscript

NIH-PA Author Manuscript

NIH-PA Author Manuscript

NIH-PA Author Manuscript

Conclusions—Targeted and sustained delivery of NRG directly to the myocardial borderzone augments cardiomyocyte mitotic activity, decreases apoptosis, and greatly enhances LV function in a model of ICM. This novel approach to NRG administration avoids off-target exposure and represents a clinically translatable strategy in myocardial regenerative therapeutics.

Keywords

myocyte; heart failure; ischemia; myocardial infarction; molecular biology

Cardiac disease is a major national health concern with approximately 15.4 million Americans suffering from coronary heart disease and 5.1 million from heart failure, while incurring an annual cost of $300 billion.[1] As interventions for acute cardiac events have evolved and become more effective, therapies aimed at mitigating the progression to heart failure have failed to keep pace. This void has led to the exploration of a variety of cell and cytokine driven vasculogenic and regenerative strategies.[2–8] Preclinical studies of these approaches have yielded promising results, while early clinical trials have been encouraging but with more modest outcomes. As a result, it is necessary to build upon these initial studies to enhance the translation to clinical therapeutics.

Neuregulin-1β (NRG) is a member of the epidermal growth factor family that plays a critical role in the development of neuronal, epithelial, and cardiac cells.[9] It is a ligand to the ErbB4 tyrosine kinase receptor, activating an intracellular signaling cascade that leads to proliferation, differentiation, and migration.[10] Importantly, the ErbB4 receptor is present in adult cardiomyocytes.[11] The significance of NRG's potential cardio-protective effects was highlighted in the clinical trials for trastuzumab (TZM), where cardiac dysfunction was a noted adverse effect.[12] TZM is a monoclonal antibody that inhibits the ErbB receptor and disrupts the NRG-ErbB signaling pathway. More recently, it has been found that TZM impairs human resident cardiac stem cells.[13] These findings support the notion that activation of the NRG-ErbB pathway critically enhances cardio-protection.

From a therapeutic perspective, NRG has shown great promise in preserving cardiac function and inducing regeneration following myocardial injury. This has been demonstrated in small and large animal models[14–18]; however, multiple systemic intravenous infusions of NRG were required. This model of multiple parenteral infusions was translated to early clinical trial where a modest benefit in acute and chronic hemodynamics was observed in patients with stable heart failure receiving daily NRG infusions for 11 days.[19] Additionally, a phase II double-blind study demonstrated improvements in LVEF and ventricular geometry utilizing daily infusions of NRG for 10 days.[20] The clear drawback of systemic NRG administration, however, is the significant potential for adverse effects and the consequent dosing limitations.

To improve upon this strategy, our group hypothesized that targeted and sustained intramyocardial delivery of NRG would yield NRG's known cardio-protective and regenerative effects, while avoiding systemic exposure and obviating the need for multiple infusions. We sought to accomplish this by utilizing an established bioengineered hydrogel system[21–24] to encapsulate NRG for sustained and localized intramyocardial delivery in a murine model of ischemic cardiomyopathy.

NIH-PA Author Manuscript

NIH-PA Author Manuscript

NIH-PA Author Manuscript

Methods

Macromer Synthesis

Sodium hyaluronate (74kDa, Lifecore) was modified with hydroxyethyl methacrylate (HEMA) to incorporate a terminal methacrylate group for free-radical initiated crosslinking and ester bonds to introduce hydrolytic degradation.[25] Briefly, HEMA was reacted with succinic anhydride via a ring opening polymerization in the presence of N-methylimidazole to obtain HEMA-COOH, which was coupled to a tetrabutylammonium salt of HA in the presence of 4-dimethylaminopyridine. The resulting HA macromer with HEMA group modification (HEMA-HA) was purified via dialysis, lyophilized, and the percentage of HA disaccharides modified with a HEMA group was determined to be ~15% using ^{1}H NMR.

Hydrogel Gelation and NRG Encapsulation with Release

To form hydrogels rapidly upon injection into myocardium, a two-component redox initiator system consisting of ammonium persulfate (APS) and N,N,N′,N′-tetramethylethylenediamine (TEMED) was utilized. APS and TEMED were added to a final concentration of 10mM in a 4% (w/v) HEMA-HA solution and kept on ice. The kinetics of gel formation were characterized with rheometry at 37°C by monitoring the storage (G') and loss (G") modulus with time, while applying oscillatory strain (20mm 1° cone geometry, 1% strain, 1Hz, Texas Instruments AR 2000ex). Recombinant human NRG-1β EGF binding domain (Thr176-Lys246) was acquired (R&D Systems, Minneapolis) and utilized for the duration of the study in the NRG alone and NRG-HG groups. For in vitro release kinetics, 2.5μg NRG was added per 50μL gel precursor solution, and 50μL gels were formed in cylindrical molds for 30 min at 37°C. Gels were incubated in 1mL PBS supplemented with 1% BSA at 37°C and buffers were refreshed every 2 days. At t=0,1,2,3,5,13,and 14 days, the supernatant was removed and the released NRG was quantified by ELISA (Abcam, Cambridge MA) to determine the percentage of total NRG released. In parallel, hydrogel degradation was quantified over 14 days with a uronic acid assay as previously described[26].

In Vitro Cardiomyocyte Isolation

Cardiomyocytes were isolated from neonatal Sprague-Dawley rat pups using a trypsin-based dissociation method as previously described[27], with minor modifications. The cell samples were centrifuged to wash away the trypsin solution and suspended in growth media composed of 4:1 ratio of DMEM and Medium-199, 10% horse serum, 5% fetal bovine serum, 1% HEPES, and 1% solution of penicillin, streptomycin, and glutamine.

The cells were pre-plated onto multiple 10mm^2 petri dishes for 1 hour to allow fibroblasts to attach to the dishes. Cardiomyocytes still suspended in the media were retained and counted. Cells were seeded onto a glass bottom 24-well plate coated with vitronectin. The seeding density for each well was 3.33×10^5 cells in 1mL of growth media. Growth media was changed 24 hours after seeding. Cells were kept in culture for 5 days so that background proliferation would subside, and were randomized into four stimulation groups: PBS alone, NRG alone, hydrogel (HG) alone, or NRG-HG. This time point is labeled as t=0 days. The media was changed daily. The hydrogels were kept suspended over the cells in a 3um pore size trans-well cell culture insert. By doing so, the daily medium changes did not wash away

NIH-PA Author Manuscript

NIH-PA Author Manuscript

NIH-PA Author Manuscript

the hydrogel, which could continue to release NRG into the fresh medium. In the NRG alone group, the NRG was not replaced after the first medium change.

Cardiomyocyte Immunohistochemistry and Confocal Microscopy

Cell proliferation was tested using immunohistochemistry at t=6 days. Wells tested using the Click-iT® EdU Imaging Kit (Life Technologies, Carlsbad CA) required incubation of the EdU reagent at t=4 days at a 1uM concentration. On t=6 days, all wells of the plate were washed with PBS and fixed with 4% paraformaldehyde. Next the cells were permeabilized using 0.5% Tween-20. Wells tested for EdU were incubated with the detection solution and washed with rinse buffer. Cells were also assayed for phosphorylated histone H3 (PH3). Cells were blocked using 10% fetal bovine serum. Primary antibody for PH3 (Abcam, Cambridge MA) was added at 1:200. Additionally, cells were stained for cardiac troponin (Abcam) at 1:200. All antibodies were suspended in PBS and the cells were incubated in solution for 2 hours at 37°C. After primary antibody incubation, the wells were washed with PBS and the secondary antibodies (ab150065 and ab150112, Abcam) were applied at 1:200 and incubated for 1 hour at 37°C. Lastly, the cells were counterstained for nuclei with DAPI (Life Technologies) and imaged using a Zeiss LSM 710 confocal microscope (Oberkochen, Germany).

Animal Care and Biosafety

Male C57BL/6 mice weighing 25–30g at 10 weeks of age were obtained from Charles River Labs (Wilmington, Massachusetts). Food and water were provided ad lib. All experiments conformed to the “Guide for the Care and Use of Laboratory Animals,” published by the US National Institutes of Health (Eighth Edition, 2011). The protocol was approved by the Institutional Animal Use and Care Committee of the University of Pennsylvania (protocol number 803190).

Animal Model

Myocardial infarction (MI) was induced in 60 mice using an established and highly reproducible model. Briefly, the mice were anesthetized in a 2L induction chamber (VetEquip, CA) and 3% isofluorane was continuously delivered. A 20-gauge angiocatheter was used for endotracheal intubation and connected to mechanical ventilation (Hallowell EMC, MA) where 2% isofluorane was maintained throughout. A thoracotomy was performed through the left 4^{th} intercostal space, the heart was exposed, and a 8-0 polypropylene suture was placed around the left anterior descending artery 2mm below the left atrium producing an anterolateral MI. The animals were randomized into 4 groups (n=13/group) and received 3 peri-infarct intramyocardial injections of either PBS (40μL), NRG alone (2.5μg in 40μL PBS), HG alone (40μL), or NRG-HG (2.5μg in 40μL HG). These borderzone injections were performed with the needle at a 20° angle to the myocardium to achieve an injection depth of 1mm avoiding intra-ventricular delivery. The thoracotomy was closed and tissue adhesive (VetBond, MN) was applied over the incision. All mice were implanted with subcutaneous microchips (BioMedic Data Systems, ID) for tracking, and recovered from anesthesia. Buprenorphine (0.5mg/kg) was administered for pain control.

NIH-PA Author Manuscript

NIH-PA Author Manuscript

NIH-PA Author Manuscript

Echocardiographic Assessment

LV geometry and function (n=32) were evaluated by echocardiography (Philips, Amsterdam) at 2 weeks following myocardial infarction and therapy. Left ventricular parasternal short axis 2D images were obtained at the papillary muscles. All analyses were performed by a single investigator who was blinded to the treatment groups.

Immunohistochemistry and Histologic Analysis

At 6 days post-operatively, a subset (n=5/group) were anesthetized as previously described, and hearts explanted. They were flushed with PBS, injected retrograde with Tissue Tek OCT (Netherlands), frozen at −80°C, and sectioned onto slides using a Leica CM3050S cryostat (Leica, Germany) at 10μm thickness. Next the samples were fixed with 4% paraformaldehyde and blocked with 10% fetal bovine serum. Sections were stained for PH3, Ki67, activated caspase-3, and NRG separately. All sections were stained for cardiac troponin. All primary antibodies (Abcam) were diluted at 1:200 in PBS and incubated for 2 hours at 37°C. Importantly, the NRG primary antibody (ab80237) was specific to the EGF binding domain of human NRG to minimize cross-reactivity with mouse neuregulin. The sections were washed in PBS and the appropriate secondary antibody was applied. The slides were washed in PBS and counterstained for nuclei with DAPI (Vector Labs). The sections were imaged with a Leica DM5000B fluorescent microscope.

For histologic analysis at 2 weeks, hearts were explanted, flushed with PBS, and injected retrograde with OCT through the aorta and pulmonary artery. Hearts were submerged in OCT, frozen, and stored in a −80°C freezer. Eight, 10μm thick sections were prepared from each heart at the papillary level and stained with Masson's Trichrome. Standardized digital photographs were taken with a Nikon D5100 SLR camera (Nikon, Japan). Photographs were uploaded to ImageJ (v1.46b) and the borderzone assessed with digital planimetry.

Peripheral Blood NRG Quantification

At 6 days following MI and therapy, a subset (n=5/group) were anesthetized, and 500μL of peripheral blood was acquired. Blood was immediately placed in a biopsy tube with EDTA to prevent clotting and flash frozen. ELISA (ab100614, Abcam) was performed on all samples to quantify levels of human NRG. The samples were read on a microplate reader (TECAN, Austria) at 450 nm.

Statistical Analysis

All analyzed variables approximated a normal distribution, and values for continuous variables were reported as means ± standard deviation. For all experiments, a Levene test was first performed to establish homogenous variance across all groups. One-way ANOVA was then performed followed by a Tukey's HSD to compare two groups at a time (α=0.05).

Results

NRG Encapsulation and Sustained Release Kinetics

NRG release was sustained for 14 days in vitro. An initial 2 day burst phase was observed where 60% of the NRG was released from the hydrogel. This was followed by a steady and

NIH-PA Author Manuscript

NIH-PA Author Manuscript

NIH-PA Author Manuscript

sustained distribution of the remaining 40% of NRG over 12 days (Figure 1A). This release pattern was consistent with previous encapsulation of other similarly sized peptides. The uronic acid assay demonstrated 100% degradation of the hydrogel over a 14 day period as well, paralleling the release of NRG (Figure 1B).

Sustained Release NRG Induces Cardiomyocyte Mitotic Activity in Vitro

Isolated cardiomyocytes were stimulated with PBS, NRG alone, HG alone, or NRG-HG at t=0 days. Importantly, trans-well plates that allowed passage of NRG released from HG were utilized, and the media was changed daily. This allowed comparison of a one-time administration of NRG versus sustained delivery. At t=6 days, the cardiomyocytes were visualized with confocal microscopy to evaluate for EdU incorporation, marking DNA synthesis. The PBS, NRG alone, and HG alone groups demonstrated no EdU incorporation compared to 10% of the cardiomyocytes in the NRG-HG group that did incorporate EdU (Figure 2A). Providing further evidence of cardiomyocyte cell-cycle activation, immunohistochemistry was performed to determine the presence of PH3. There was no PH3 observed in the PBS, NRG alone, and HG alone groups, while the NRG-HG group exhibited PH3 positivity (Figure 2B) in 2% of the cardiomyocytes.

Sustained Release NRG Induces Cardiomyocyte Mitotic Activity in Vivo

At 6 days post-operatively, hearts were explanted for immunohistochemistry (n=5/group) and determination of the presence of PH3 and Ki67. Heart sections in the three controls groups did not demonstrate evidence of PH3 or Ki67. In all of the NRG-HG treated animals, heart sections were positive for PH3 and Ki67 (Figure 3A and 3B).

Sustained Release NRG Provides Cardio-protection in Vivo

In the same subset at 6 days post-surgery, heart sections (n=5/group) were evaluated by immunohistochemistry for the presence of activated caspase-3, a mediator of apoptosis and parameter of cardio-protection[28]. This was quantified by number of positive cells per 10× high powered field. The PBS (5.6±0.8 cells;p=0.005), and HG (6.2±0.97 cells; p=0.006) groups demonstrated significantly higher levels of activated caspase-3 compared to the NRG-HG group (1.5±0.29 cells) (Figure 4). The NRG group demonstrated a greater number of positive cells (3.5±0.29 cells) compared to NRG-HG, but was not statistically significant.

Encapsulated NRG in Hydrogel Provides Sustained Local Release in Vivo without Peripheral Exposure

In the same subset at 6 days post-surgery, peripheral blood (n=5/group) was acquired along with explanted hearts. Immunohistochemistry of explanted hearts demonstrated the presence of NRG in the myocardium in the NRG-HG group only (Figure 5A). The peripheral blood was assessed for the presence of NRG. There was no difference in peripheral blood NRG levels throughout all groups: Native (3.6±0.4 ng/mL; p>0.5), NRG (3.4±0.3 ng/mL; p>0.5), HG (3.1±0.2 ng/mL; p>0.5), NRG-HG (3.5±0.2 ng/mL) (Figure 5B).

NIH-PA Author Manuscript

NIH-PA Author Manuscript

NIH-PA Author Manuscript

Echocardiographic Assessment

At 14 days post-operatively, the animals were anesthetized and were evaluated by echocardiography (n=8/group). LV chamber area at the level of the papillary muscles was analyzed. The PBS (0.29 cm^2±0.02 cm^2; p=0.05), NRG alone (0.33 cm^2±0.04 cm^2; p=0.02), and HG alone (0.26 cm^2±0.05 cm^2; p=0.03) animals all demonstrated significantly greater LV chamber areas compared to NRG-HG treated animals (0.18 cm^2±0.02 cm^2) (Figure 6A). Additionally, LVEF was determined at 14 days. The PBS (20.2%±3.2%; p<0.01), NRG alone (20.1%±4.7%; p<0.01), and HG alone (17.2%±3.7%; p<0.01) groups all exhibited significantly reduced LVEF compared to NRG-HG treated animals (37.5%±3.6%) (Figure 6B).

Histologic Evaluation

Directly following ECHO evaluation at 14 days, hearts were explanted and frozen sections were acquired for histologic analysis (n=8/group). Masson's Trichrome staining was performed to evaluate borderzone thickness. The PBS (0.27 mm±0.04 mm; p<0.01), NRG alone (0.30 mm±0.05 mm; p<0.01), and HG alone (0.26 mm±0.05 mm; p<0.01) groups revealed a significantly reduced borderzone thickness compared to animals receiving NRG-HG (0.65 mm±0.07 mm) (Figure 7).

Discussion

This study demonstrated that localized and sustained myocardial delivery of NRG stimulates cardiomyocyte mitotic activity, provides cardio-protection, reduces LV dilation, and enhances ventricular function in a murine model of ischemic cardiomyopathy. The novel and integral component of this study was the encapsulation of NRG in the hydrogel delivery system. While previous preclinical and clinical studies have revealed a functional benefit of repeated systemic dosing of NRG, there remains a legitimate concern regarding NRG's potential oncologic consequences and its effect on the nervous system.[29] The locally administered encapsulated NRG addresses this problem, allows for greater flexibility in dosing, and obviates the requirement for daily infusions. A crucial component of this study was confirming the presence of the administered NRG in the myocardium 6 days following injection only when delivered in a hydrogel. Additionally, analysis of the peripheral blood at this time-point exhibited no difference in NRG levels throughout all groups, including native mice. The very low levels of NRG detected were probably due to minimal cross-reactivity between the detection antibody and native mouse neuregulin. These findings strongly support the strategy of sustained and local NRG delivery to the myocardium with minimal off-target exposure.

Over the last decade, a multitude of bioengineered systems have been developed as adjuncts to cytokine, peptide, and cell therapies for heart failure. These include but are not limited to cell-sheets[30–32], fibrin patches[33, 34], alginate scaffolds[35, 36], and hydrogels[25, 37–39]. The hyaluronic acid hydrogel was utilized in this study because of its previous effectiveness in encapsulating similarly sized peptides and its demonstrated safety in humans.[40, 41] There is strong evidence to suggest that administration of hydrogel alone contributes to cardiac repair and improvement in function[21, 42]; however, this was not observed in this study. The most

NIH-PA Author Manuscript

NIH-PA Author Manuscript

NIH-PA Author Manuscript

logical explanation is that a very small volume of 40μL was injected into the myocardium. This volume was optimal for encapsulating the determined dose of 2.5μg of NRG and treating the borderzone. Since the focus of the study was to evaluate localized and sustained release of NRG, we optimized hydrogel volume and macromer density for this purpose. It is possible that a greater volume of hydrogel would yield a benefit in itself.

Following encapsulation of NRG, it was critical to determine that NRG could be released from the gel over an extended period of time without hindering its function. This was accomplished by incubating the NRG containing hydrogel in PBS and evaluating the supernatant by ELISA over 14 days. The typical burst phase was observed followed by a steady release of NRG. Following this analysis, in vitro experiments on isolated cardiomyocytes demonstrated that the released NRG retained its ability to activate the ErBb signaling axis. Importantly, these experiments were carefully performed such that the cells were cultured on a trans-well plate where the hydrogel was suspended above the cells. This allowed for daily medium changes while keeping the hydrogel in place and continually releasing NRG into the new medium. In the NRG alone group, the NRG was not replaced after the first medium change. This allowed comparison between cardiomyocytes undergoing sustained NRG stimulation versus a one-time stimulation. The data demonstrated that activation of the cardiomyocyte cell-cycle occurred only with sustained NRG administration. The NRG dosing was based on a previous study which characterized differentiated cardiomyocyte cell-cycle reentry following multiple days of NRG stimulation,[14] which was consistent with this study's findings. The visualization of EdU incorporation and PH3 positivity in NRG-HG stimulated cells strongly supports that the integrity of the NRG-ErBb signaling axis was maintained.

After demonstration that NRG retains activity following hydrogel release, findings of reduced LV dilation and significantly improved LVEF coupled with increased borderzone thickness on histology 2 weeks following therapy illustrate enhancement of ventricular function and structure resulting from NRG-HG therapy. The in vitro and in vivo data exhibiting cardiomyocyte mitotic activity support the notion that NRG-HG induced cardiomyocyte regeneration contributed to enhanced ventricular function. The decreased levels of activated caspase-3 following NRG-HG treatment also suggests an anti-apoptotic effect. It is logical that NRG administration would yield a protective effect in conjunction with a regenerative stimulus as the downstream pathway of the ErbB receptors includes PI3K and Akt, which are well-established mediators of cellular proliferation and protection.[43] It is possible that additional mechanisms of action such as inotropy are involved. NRG has been determined to modulate nitric oxide synthesis and affect cardiomyocyte calcium cycling[44]; however, multiple studies have actually concluded NRG has a slightly negative inotropic effect.[45, 46] Additionally, the role of cardiac stem cells and NRG's interaction with them was not studied here. Previous work has somewhat elucidated this mechanism where fate mapping experiments showed NRG induced cardiomyocyte regeneration occurred with already differentiated cardiomyocytes.[14]

There were limitations to the study. While the experiments confirmed the presence of NRG in the myocardium 6 days following injection, further information concerning the kinetics of encapsulated NRG administration would be helpful. This could be accomplished in future

NIH-PA Author Manuscript

NIH-PA Author Manuscript

NIH-PA Author Manuscript

experiments by conjugating a fluorophore to NRG and utilizing serial optical imaging to track its location over time. Regarding limitations involving delivery, intramyocardial injection poses a manageable hurdle when translating to clinical application. In addition to being an adjunct to cardiac surgery, hydrogels that are more suitable for catheter-based administration are being explored.[47] As a result, the translational potential of this therapy is greatly broadened.

Overall, this study demonstrated that targeted and sustained delivery of NRG to borderzone myocardium stimulates cardiomyocyte mitotic activity, cardio-protection, and significantly enhances ventricular function and structure. It is an extremely translatable therapy in that it addresses a major national health concern, NRG alone has reached clinical trial in the setting of systemic administration, and hyaluronic acid hydrogels have been shown to be safe in humans. This novel method of utilizing a bioengineered hydrogel for targeted intramyocardial NRG delivery warrants further evaluation in a preclinical model.

Acknowledgments

Sources of Funding

This work was supported in part by funding from NIH R01 HL089315 (Woo).

References

1. Go AS, Mozaffarian D, Roger VL, Benjamin EJ, Berry JD, Borden WB, Bravata DM, Dai S, Ford ES, Fox CS, Franco S, Fullerton HJ, Gillespie C, Hailpern SM, Heit JA, Howard VJ, Huffman MD, Kissela BM, Kittner SJ, Lackland DT, Lichtman JH, Lisabeth LD, Magid D, Marcus GM, Marelli A, Matchar DB, McGuire DK, Mohler ER, Moy CS, Mussolino ME, Nichol G, Paynter NP, Schreiner PJ, Sorlie PD, Stein J, Turan TN, Virani SS, Wong ND, Woo D, Turner MB. American Heart Association Statistics C, Stroke Statistics S. Executive summary: Heart disease and stroke statistics--2013 update: A report from the american heart association. Circulation. 2013; 127:143–152. [PubMed: 23283859]
2. Chugh AR, Beache GM, Loughran JH, Mewton N, Elmore JB, Kajstura J, Pappas P, Tatooles A, Stoddard MF, Lima JA, Slaughter MS, Anversa P, Bolli R. Administration of cardiac stem cells in patients with ischemic cardiomyopathy: The scipio trial: Surgical aspects and interim analysis of myocardial function and viability by magnetic resonance. Circulation. 2012; 126:S54–S64. [PubMed: 22965994]
3. Sanganalmath SK, Bolli R. Cell therapy for heart failure: A comprehensive overview of experimental and clinical studies, current challenges, and future directions. Circulation research. 2013; 113:810–834. [PubMed: 23989721]
4. Hiesinger W, Perez-Aguilar JM, Atluri P, Marotta NA, Frederick JR, Fitzpatrick JR 3rd, McCormick RC, Muenzer JR, Yang EC, Levit RD, Yuan LJ, Macarthur JW, Saven JG, Woo YJ. Computational protein design to reengineer stromal cell-derived factor-1alpha generates an effective and translatable angiogenic polypeptide analog. Circulation. 2011; 124:S18–S26. [PubMed: 21911811]
5. Honold J, Fischer-Rasokat U, Lehmann R, Leistner DM, Seeger FH, Schachinger V, Martin H, Dimmeler S, Zeiher AM, Assmus B. G-csf stimulation and coronary reinfusion of mobilized circulating mononuclear proangiogenic cells in patients with chronic ischemic heart disease:Five-year results of the topcare-g-csf trial. Cell transplantation. 2012; 21:2325–2337. [PubMed: 22963750]
6. Bolli R, Tang XL, Sanganalmath SK, Rimoldi O, Mosna F, Abdel-Latif A, Jneid H, Rota M, Leri A, Kajstura J. Intracoronary delivery of autologous cardiac stem cells improves cardiac function in a porcine model of chronic ischemic cardiomyopathy. Circulation. 2013; 128:122–131. [PubMed: 23757309]

NIH-PA Author Manuscript

NIH-PA Author Manuscript

NIH-PA Author Manuscript

7. Surder D, Manka R, Lo Cicero V, Moccetti T, Rufibach K, Soncin S, Turchetto L, Radrizzani M, Astori G, Schwitter J, Erne P, Zuber M, Auf der Maur C, Jamshidi P, Gaemperli O, Windecker S, Moschovitis A, Wahl A, Buhler I, Wyss C, Kozerke S, Landmesser U, Luscher TF, Corti R. Intracoronary injection of bone marrow-derived mononuclear cells early or late after acute myocardial infarction: Effects on global left ventricular function. Circulation. 2013; 127:1968–1979. [PubMed: 23596006]
8. Leistner DM, Fischer-Rasokat U, Honold J, Seeger FH, Schachinger V, Lehmann R, Martin H, Burck I, Urbich C, Dimmeler S, Zeiher AM, Assmus B. Transplantation of progenitor cells and regeneration enhancement in acute myocardial infarction (topcareami): Final 5-year results suggest long-term safety and efficacy. Clinical research in cardiology. 2011; 100:925–934. [PubMed: 21633921]
9. Wadugu B, Kuhn B. The role of neuregulin/erbb2/erbb4 signaling in the heart with special focus on effects on cardiomyocyte proliferation. American journal of physiology. Heart and circulatory physiology. 2012; 302:H2139–H2147. [PubMed: 22427524]
10. Citri A, Yarden Y. Egf-erbb signalling: Towards the systems level. Nature reviews. Molecular cell biology. 2006; 7:505–516.
11. Zhao YY, Sawyer DR, Baliga RR, Opel DJ, Han X, Marchionni MA, Kelly RA. Neuregulins promote survival and growth of cardiac myocytes. Persistence of erbb2 and erbb4 expression in neonatal and adult ventricular myocytes. The Journal of biological chemistry. 1998; 273:10261–10269. [PubMed: 9553078]
12. Jerian S, Keegan P. Cardiotoxicity associated with paclitaxel/trastuzumab combination therapy. Journal of clinical oncology. 1999; 17:1647–1648. [PubMed: 10334560]
13. Barth AS, Zhang Y, Li T, Smith RR, Chimenti I, Terrovitis I, Davis DR, Kizana E, Ho AS, O'Rourke B, Wolff AC, Gerstenblith G, Marban E. Functional impairment of human resident cardiac stem cells by the cardiotoxic antineoplastic agent trastuzumab. Stem cells translational medicine. 2012; 1:289–297. [PubMed: 23197808]
14. Bersell K, Arab S, Haring B, Kuhn B. Neuregulin1/erbb4 signaling induces cardiomyocyte proliferation and repair of heart injury. Cell. 2009; 138:257–270. [PubMed: 19632177]
15. Bian Y, Sun M, Silver M, Ho KK, Marchionni MA, Caggiano AO, Stone JR, Amende I, Hampton TG, Morgan JP, Yan X. Neuregulin-1 attenuated doxorubicin-induced decrease in cardiac troponins. American journal of physiology. Heart and circulatory physiology. 2009; 297:H1974–H1983. [PubMed: 19801490]
16. Gu X, Liu X, Xu D, Li X, Yan M, Qi Y, Yan W, Wang W, Pan J, Xu Y, Xi B, Cheng L, Jia J, Wang K, Ge J, Zhou M. Cardiac functional improvement in rats with myocardial infarction by up-regulating cardiac myosin light chain kinase with neuregulin. Cardiovascular research. 2010; 88:334–343. [PubMed: 20615916]
17. Guo YF, Zhang XX, Liu Y, Duan HY, Jie BZ, Wu XS. Neuregulin-1 attenuates mitochondrial dysfunction in a rat model of heart failure. Chinese medical journal. 2012; 125:807–814. [PubMed: 22490579]
18. Liu X, Gu X, Li Z, Li X, Li H, Chang J, Chen P, Jin J, Xi B, Chen D, Lai D, Graham RM, Zhou M. Neuregulin-1/erbb-activation improves cardiac function and survival in models of ischemic, dilated, and viral cardiomyopathy. Journal of the American College of Cardiology. 2006; 48:1438–1447. [PubMed: 17010808]
19. Jabbour A, Hayward CS, Keogh AM, Kotlyar E, McCrohon JA, England JF, Amor R, Liu X, Li XY, Zhou MD, Graham RM, Macdonald PS. Parenteral administration of recombinant human neuregulin-1 to patients with stable chronic heart failure produces favourable acute and chronic haemodynamic responses. European journal of heart failure. 2011; 13:83–92. [PubMed: 20810473]
20. Gao R, Zhang J, Cheng L, Wu X, Dong W, Yang X, Li T, Liu X, Xu Y, Li X, Zhou M. A phase ii, randomized, double-blind, multicenter, based on standard therapy, placebo-controlled study of the efficacy and safety of recombinant human neuregulin-1 in patients with chronic heart failure. Journal of the American College of Cardiology. 2010; 55:1907–1914. [PubMed: 20430261]
21. Tous E, Ifkovits JL, Koomalsingh KJ, Shuto T, Soeda T, Kondo N, Gorman JH 3rd, Gorman RC, Burdick JA. Influence of injectable hyaluronic acid hydrogel degradation behavior on infarction-induced ventricular remodeling. Biomacromolecules. 2011; 12:4127–4135. [PubMed: 21967486]

NIH-PA Author Manuscript

NIH-PA Author Manuscript

NIH-PA Author Manuscript

22. Burdick JA, Murphy WL. Moving from static to dynamic complexity in hydrogel design. Nature communications. 2012; 3:1269.

23. Hanjaya-Putra D, Wong KT, Hirotsu K, Khetan S, Burdick JA, Gerecht S. Spatial control of cell-mediated degradation to regulate vasculogenesis and angiogenesis in hyaluronan hydrogels. Biomaterials. 2012; 33:6123–6131. [PubMed: 22672833]

24. MacArthur JW Jr, Purcell BP, Shudo Y, Cohen JE, Fairman A, Trubelja A, Patel J, Hsiao P, Yang E, Lloyd K, Hiesinger W, Atluri P, Burdick JA, Woo YJ. Sustained release of engineered stromal cell-derived factor 1-alpha from injectable hydrogels effectively recruits endothelial progenitor cells and preserves ventricular function after myocardial infarction. Circulation. 2013; 128:S79–S86. [PubMed: 24030424]

25. Purcell BP, Elser JA, Mu A, Margulies KB, Burdick JA. Synergistic effects of sdf-1alpha chemokine and hyaluronic acid release from degradable hydrogels on directing bone marrow derived cell homing to the myocardium. Biomaterials. 2012; 33:7849–7857. [PubMed: 22835643]

26. Bitter T, Muir HM. A modified uronic acid carbazole reaction. Analytical biochemistry. 1962; 4:330–334. [PubMed: 13971270]

27. Simpson P, Savion S. Differentiation of rat myocytes in single cell cultures with and without proliferating nonmyocardial cells. Cross-striations, ultrastructure, and chronotropic response to isoproterenol. Circulation research. 1982; 50:101–116. [PubMed: 7053872]

28. Zhao J, Wang F, Zhang Y, Jiao L, Lau WB, Wang L, Liu B, Gao E, Koch WJ, Ma XL, Wang Y. Sevoflurane preconditioning attenuates myocardial ischemia/reperfusion injury via caveolin-3-dependent cyclooxygenase-2 inhibition. Circulation. 2013; 128:S121–S129. [PubMed: 24030395]

29. Odiete O, Hill MF, Sawyer DB. Neuregulin in cardiovascular development and disease. Circulation research. 2012; 111:1376–1385. [PubMed: 23104879]

30. Kawamura M, Miyagawa S, Fukushima S, Saito A, Miki K, Ito E, Sougawa N, Kawamura T, Daimon T, Shimizu T, Okano T, Toda K, Sawa Y. Enhanced survival of transplanted human induced pluripotent stem cell-derived cardiomyocytes by the combination of cell sheets with the pedicled omental flap technique in a porcine heart. Circulation. 2013; 128:S87–S94. [PubMed: 24030425]

31. Shudo Y, Cohen JE, Macarthur JW, Atluri P, Hsiao PF, Yang EC, Fairman AS, Trubelja A, Patel J, Miyagawa S, Sawa Y, Woo YJ. Spatially oriented, temporally sequential smooth muscle cell-endothelial progenitor cell bi-level cell sheet neovascularizes ischemic myocardium. Circulation. 2013; 128:S59–S68. [PubMed: 24030422]

32. Shudo Y, Miyagawa S, Ohkura H, Fukushima S, Saito A, Shiozaki M, Kawaguchi N, Matsuura N, Shimizu TMP, Okano TPD, Matsuyama A, Sawa Y. Addition of mesenchymal stem cells enhances the therapeutic effects of skeletal myoblast cell-sheet transplantation in a rat ischemic cardiomyopathy model. Tissue engineering. Part A. 2013; 20:728–739. [PubMed: 24164292]

33. Bago JR, Soler-Botija C, Casani L, Aguilar E, Alieva M, Rubio N, Bayes-Genis A, Blanco J. Bioluminescence imaging of cardiomyogenic and vascular differentiation of cardiac and subcutaneous adipose tissue-derived progenitor cells in fibrin patches in a myocardium infarct model. International journal of cardiology. 2013; 169:288–295. [PubMed: 24157237]

34. Ye L, Zhang P, Duval S, Su L, Xiong Q, Zhang J. Thymosin beta4 increases the potency of transplanted mesenchymal stem cells for myocardial repair. Circulation. 2013; 128:S32–S41. [PubMed: 24030419]

35. Ruvinov E, Leor J, Cohen S. The promotion of myocardial repair by the sequential delivery of igf-1 and hgf from an injectable alginate biomaterial in a model of acute myocardial infarction. Biomaterials. 2011; 32:565–578. [PubMed: 20889201]

36. Yu J, Du KT, Fang Q, Gu Y, Mihardja SS, Sievers RE, Wu JC, Lee RJ. The use of human mesenchymal stem cells encapsulated in rgd modified alginate microspheres in the repair of myocardial infarction in the rat. Biomaterials. 2010; 31:7012–7020. [PubMed: 20566215]

37. Burdick JA, Mauck RL, Gorman JH 3rd, Gorman RC. Acellular biomaterials: An evolving alternative to cell-based therapies. Science translational medicine. 2013; 5 176ps174.

38. Dhingra S, Li P, Huang XP, Guo J, Wu J, Mihic A, Li SH, Zang WF, Shen D, Weisel RD, Singal PK, Li RK. Preserving prostaglandin e2 level prevents rejection of implanted allogeneic

NIH-PA Author Manuscript

NIH-PA Author Manuscript

NIH-PA Author Manuscript

mesenchymal stem cells and restores postinfarction ventricular function. Circulation. 2013; 128:S69–S78. [PubMed: 24030423]

39. Khetan S, Guvendiren M, Legant WR, Cohen DM, Chen CS, Burdick JA. Degradation-mediated cellular traction directs stem cell fate in covalently crosslinked three-dimensional hydrogels. Nature materials. 2013; 12:458–465.
40. Chang KV, Hsiao MY, Chen WS, Wang TG, Chien KL. Effectiveness of intra-articular hyaluronic acid for ankle osteoarthritis treatment: A systematic review and meta-analysis. Archives of physical medicine and rehabilitation. 2013; 94:951–960. [PubMed: 23149311]
41. Chareancholvanich K, Pornrattanamaneewong C, Narkbunnam R. Increased cartilage volume after injection of hyaluronic acid in osteoarthritis knee patients who underwent high tibial osteotomy. Knee surgery, sports traumatology, arthroscopy. 2013; 22:1415–1423.
42. Kichula ET, Wang H, Dorsey SM, Szczesny SE, Elliott DM, Burdick JA, Wenk JF. Experimental and computational investigation of altered mechanical properties in myocardium after hydrogel injection. Ann Biomed Eng. 2013 Nov 23. [Epub ahead of print].
43. Milano G, Abruzzo PM, Bolotta A, Marini M, Terraneo L, Ravara B, Gorza L, Vitadello M, Burattini S, Curzi D, Falcieri E, von Segesser LK, Samaja M. Impact of the phosphatidylinositide 3-kinase signaling pathway on the cardioprotection induced by intermittent hypoxia. PloS one. 2013; 8:e76659. [PubMed: 24124584]
44. Brero A, Ramella R, Fitou A, Dati C, Alloatti G, Gallo MP, Levi R. Neuregulin-1beta1 rapidly modulates nitric oxide synthesis and calcium handling in rat cardiomyocytes. Cardiovascular research. 2010; 88:443–452. [PubMed: 20634213]
45. Lemmens K, Fransen P, Sys SU, Brutsaert DL, De Keulenaer GW. Neuregulin-1 induces a negative inotropic effect in cardiac muscle: Role of nitric oxide synthase. Circulation. 2004; 109:324–326. [PubMed: 14732742]
46. Okoshi K, Nakayama M, Yan X, Okoshi MP, Schuldt AJ, Marchionni MA, Lorell BH. Neuregulins regulate cardiac parasympathetic activity: Muscarinic modulation of beta-adrenergic activity in myocytes from mice with neuregulin-1 gene deletion. Circulation. 2004; 110:713–717. [PubMed: 15289373]
47. Rodell CB, Kaminski AL, Burdick JA. Rational design of network properties in guesthost assembled and shear-thinning hyaluronic acid hydrogels. Biomacromolecules. 2013; 14:4125–4134. [PubMed: 24070551]

NIH-PA Author Manuscript

NIH-PA Author Manuscript

NIH-PA Author Manuscript

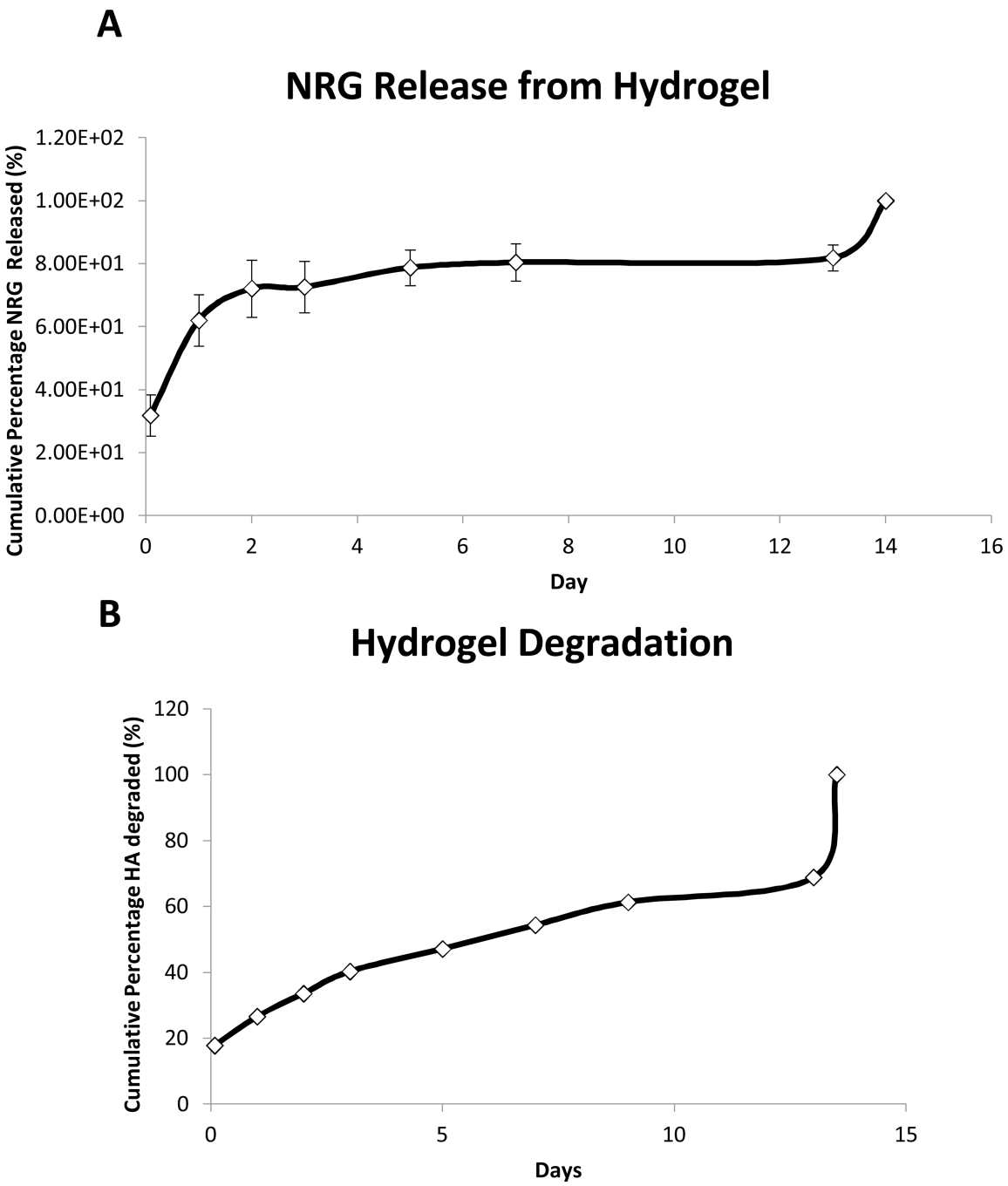

Figure 1. Sustained NRG secretion

Release kinetics of NRG from hydrogel are demonstrated over 14 days. The typical burst phase of 60% release over 2 days is demonstrated followed by sustained release for 14 days(A). The degradation of the hydrogel is displayed by quantifying uronic acid levels over 14 days (B).

NIH-PA Author Manuscript
NIH-PA Author Manuscript
NIH-PA Author Manuscript

A

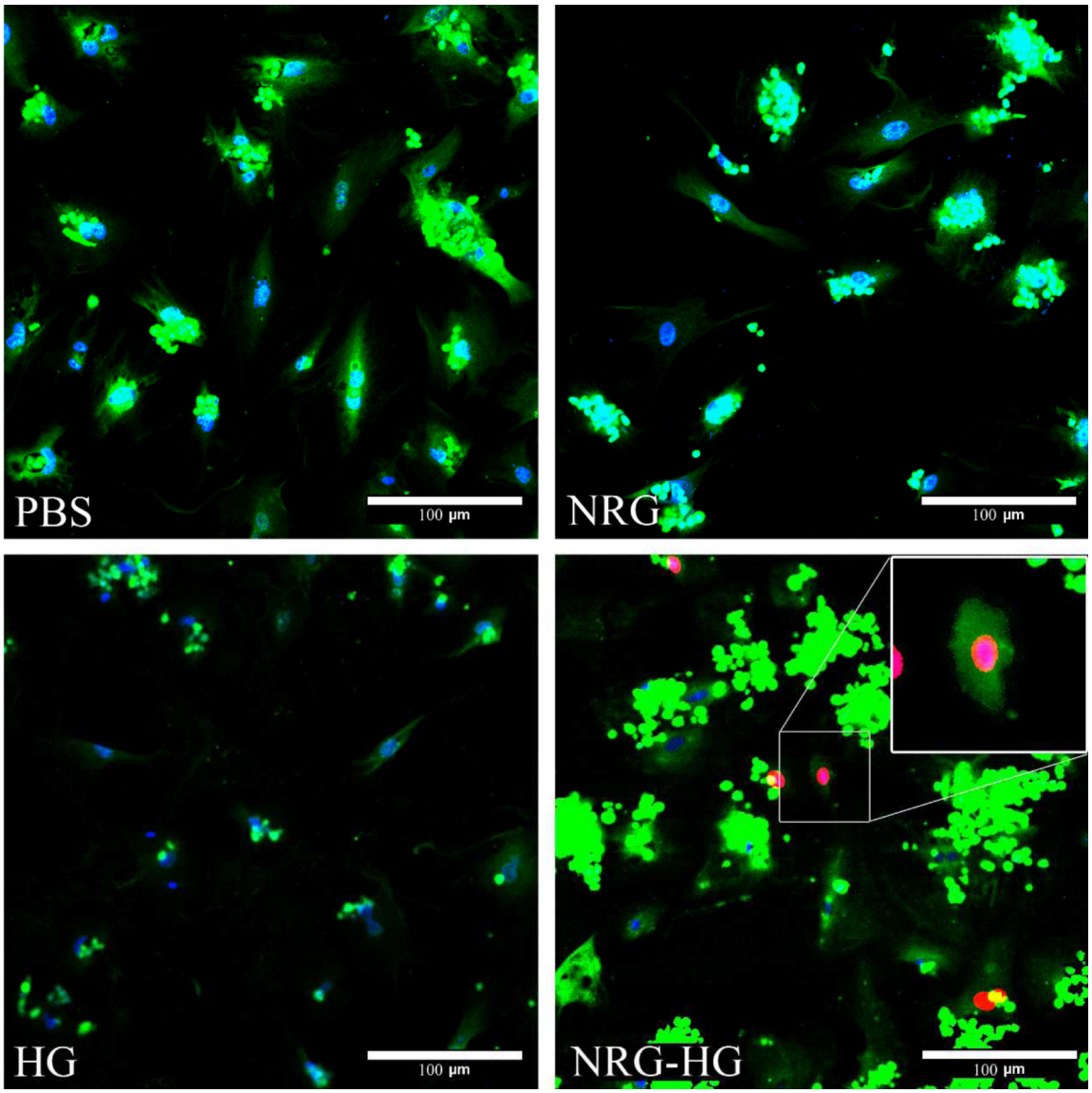

NIH-PA Author Manuscript
NIH-PA Author Manuscript
NIH-PA Author Manuscript

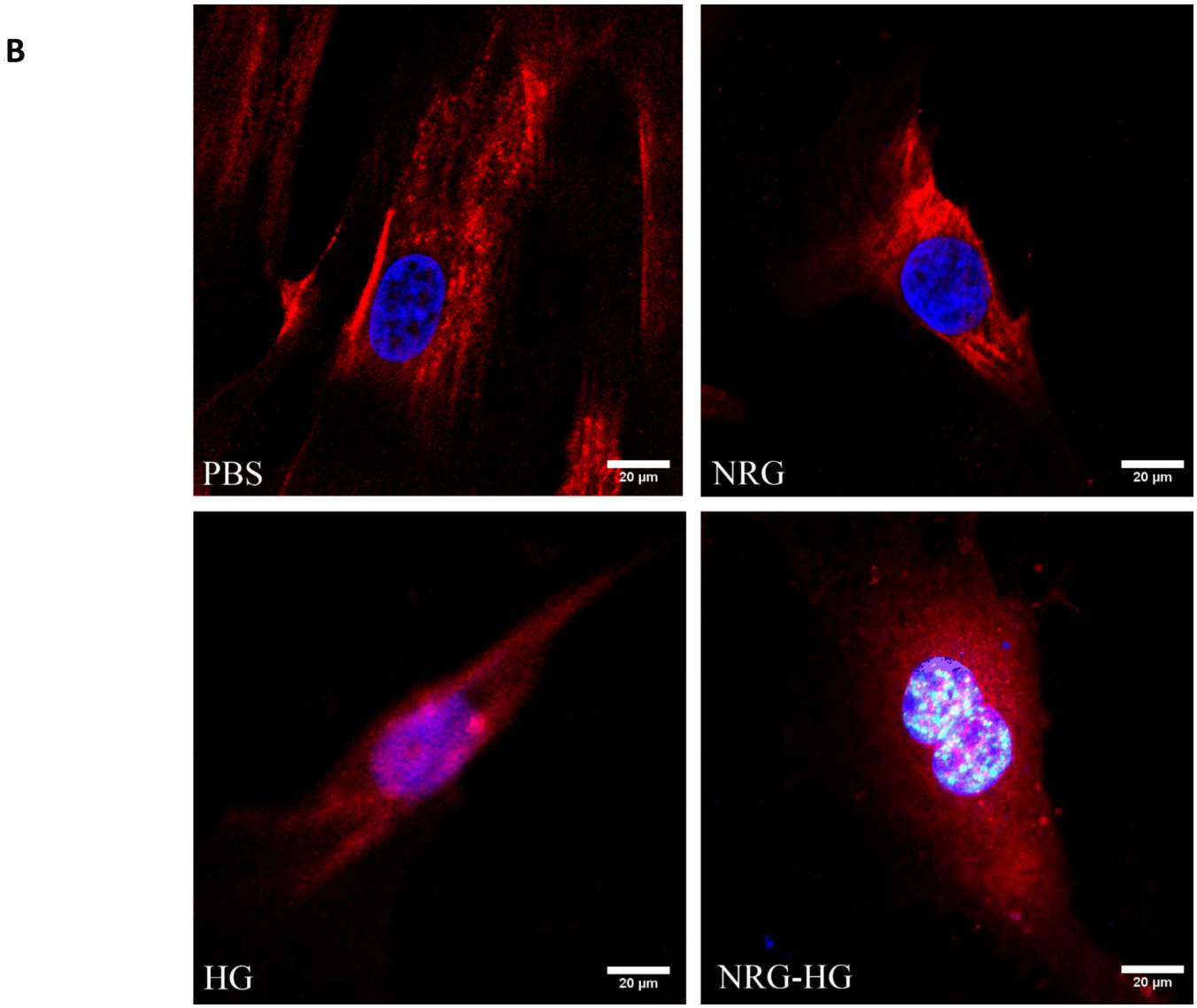

Figure 2. Cardiomyocyte mitotic activity

Confocal microscopy illustrating EdU incorporation and PH3 in isolated cardiomyocytes 6 days following stimulation. Cells are stained with DAPI (blue), troponin (green), and EdU (red). 10% of NRG-HG treated cardiomyocytes were positive for EdU incorporation. A higher magnification view is provided for the EdU positive cardiomyocyte (A). For PH3 staining, cells are stained with DAPI (blue), troponin (red), and PH3 (green). 2% of NRG-HG treated cardiomyocytes were positive for PH3 (B).

NIH-PA Author Manuscript
NIH-PA Author Manuscript
NIH-PA Author Manuscript

A

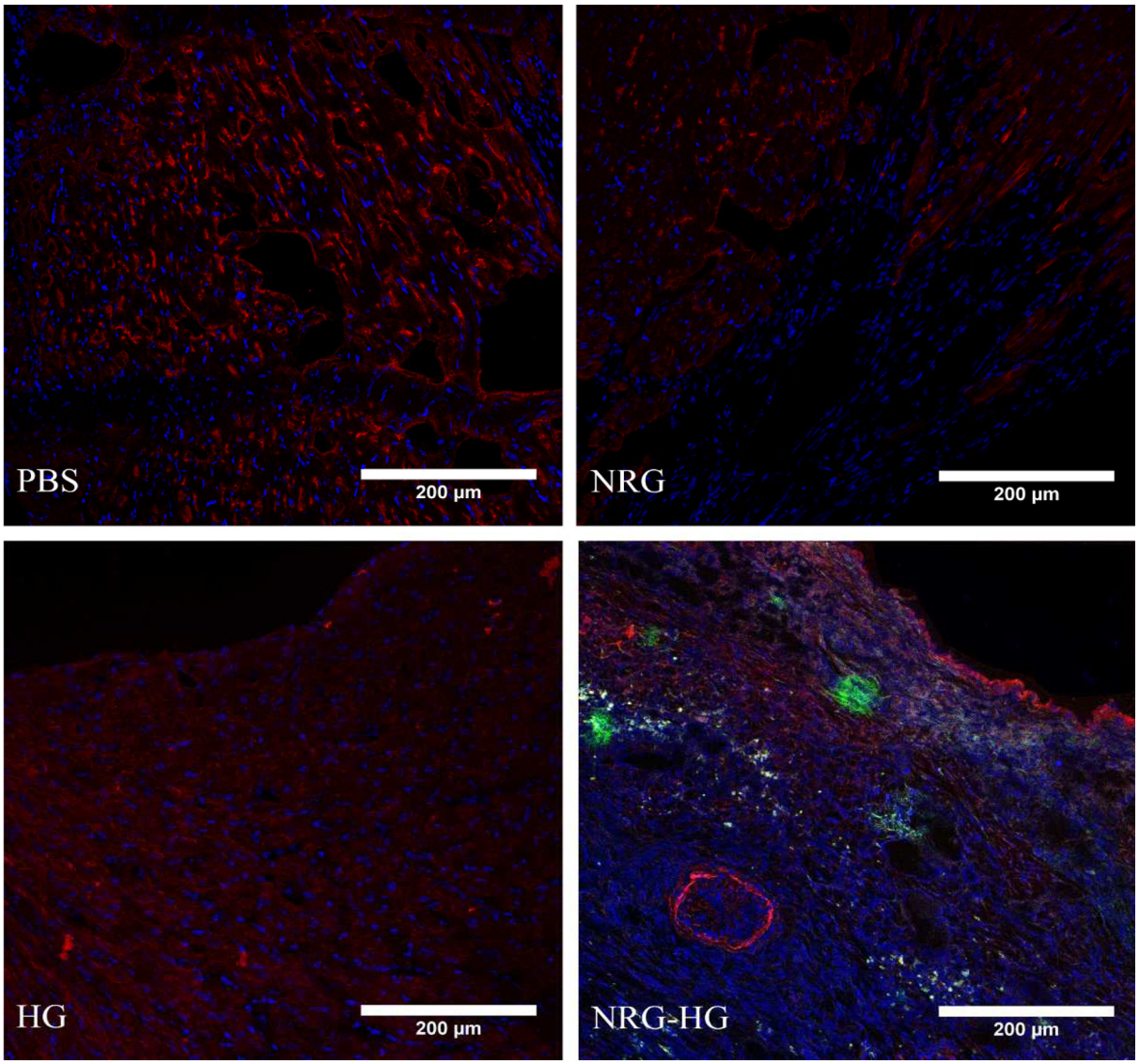

NIH-PA Author Manuscript
NIH-PA Author Manuscript
NIH-PA Author Manuscript

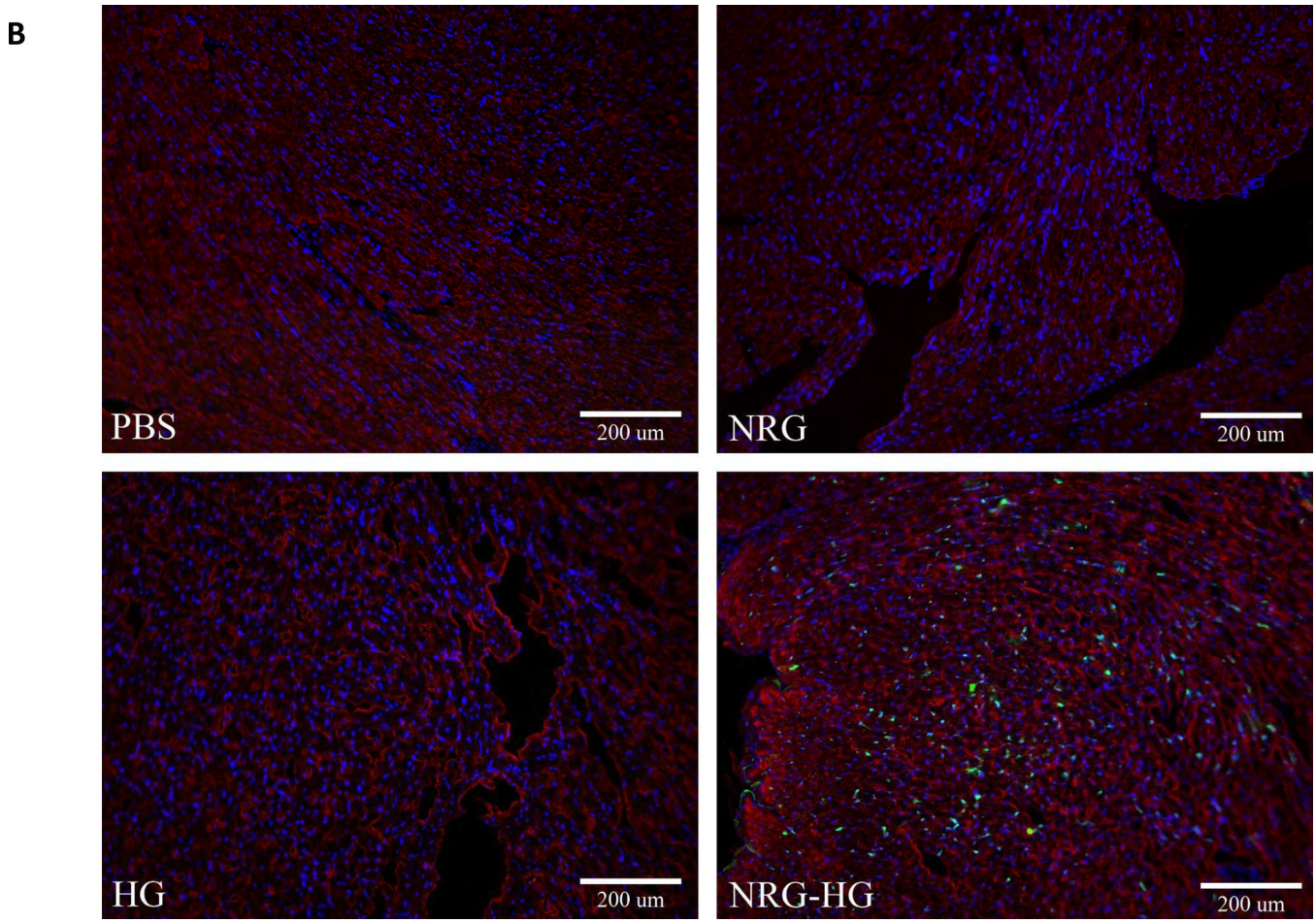

Figure 3. Mitotic activity in peri-infarct region

Heart sections at 6 days following treatment visualized under fluorescent microscopy demonstrating PH3 and Ki67 positivity with NRG-HG treatment. Sections are stained with DAPI (blue), troponin (red), PH3 (A) and Ki67 (B) (green). All animals treated with NRG-HG demonstrated presence of PH3 and Ki67 in the peri-infarct region.

NIH-PA Author Manuscript

NIH-PA Author Manuscript

NIH-PA Author Manuscript

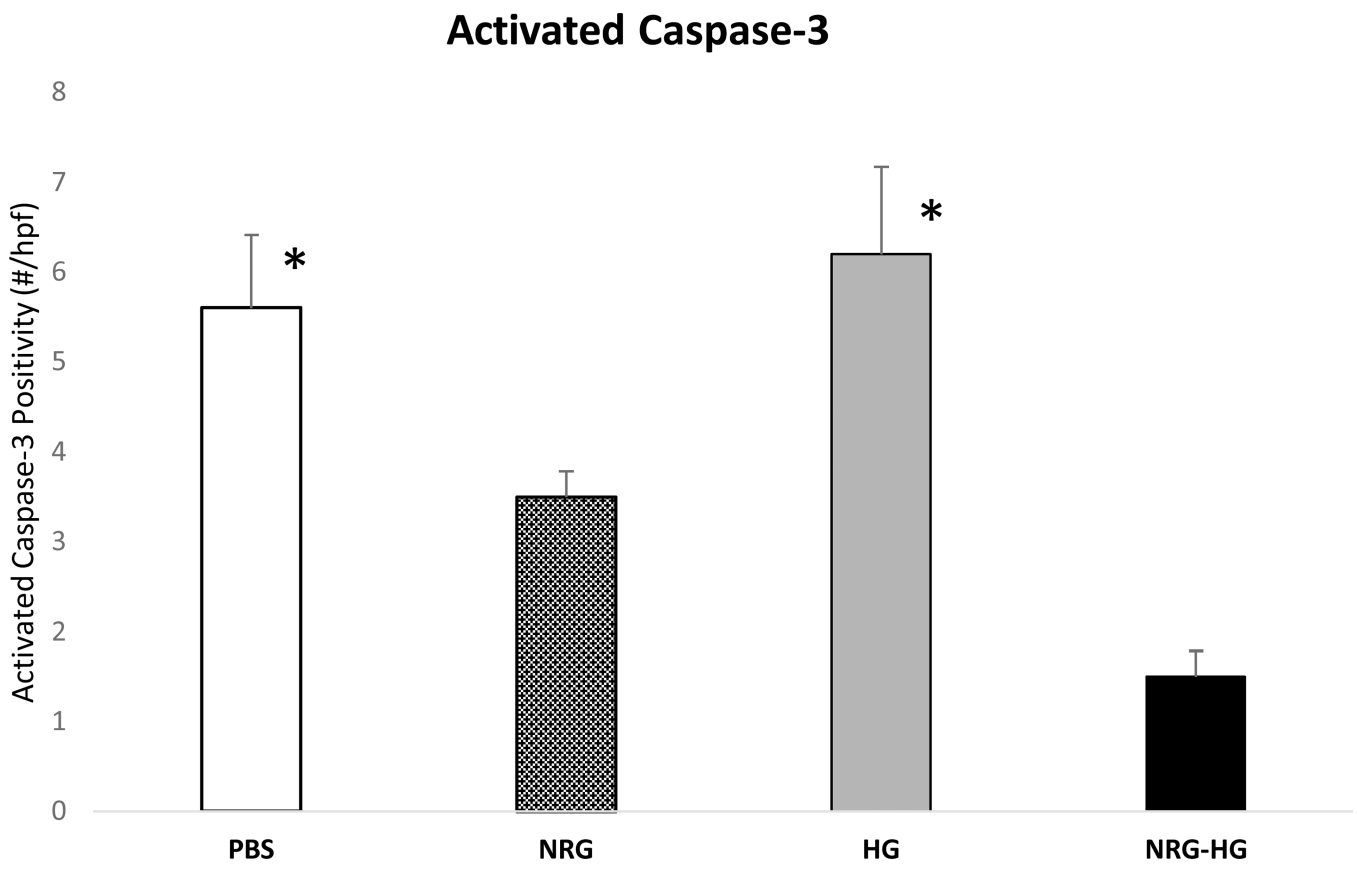

Figure 4. Cardio-protective effect of NRG-HG

Graph demonstrating significantly decreased levels of activated caspase-3 in NRG-HG treated animals compared to PBS and HG groups (* denotes $p<0.05$ for each group vs. NRG-HG).

NIH-PA Author Manuscript
NIH-PA Author Manuscript
NIH-PA Author Manuscript

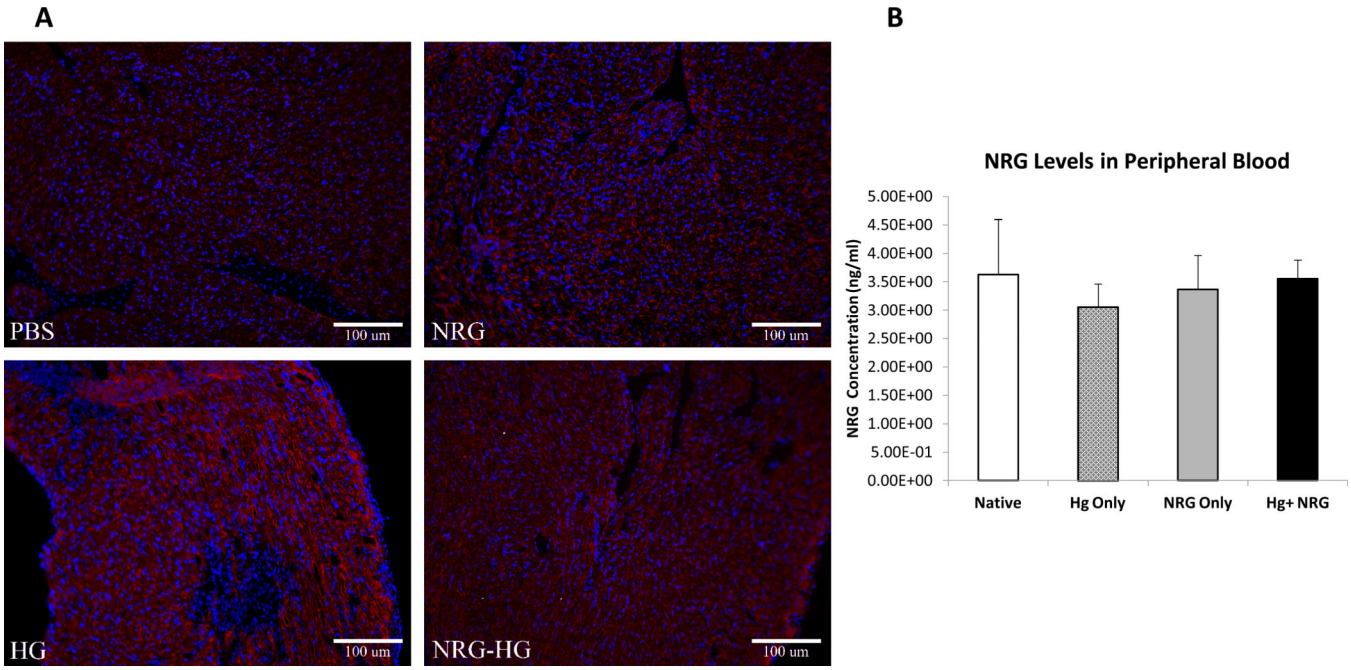

Figure 5. Sustained local delivery of NRG without off-target exposure

Heart sections 6 days following intramyocardial injection demonstrating the presence of NRG in the myocardium in the NRG-HG group only (A). Sections are stained with DAPI (blue), troponin (red), and NRG (green). ELISA performed on peripheral blood quantifying NRG levels 6 days following injection. There was no significant difference in NRG levels between groups (B).

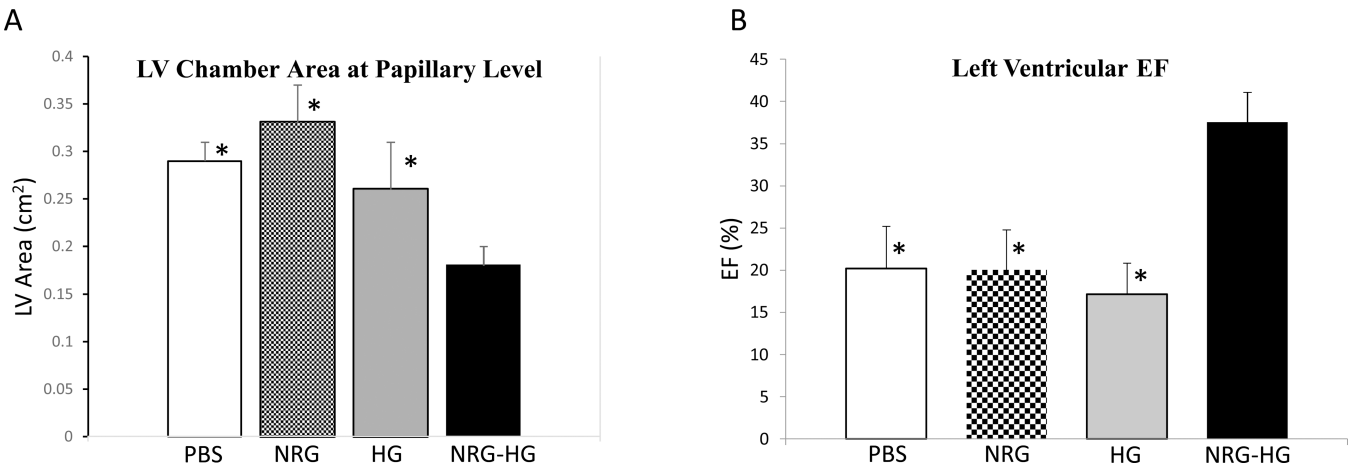

Figure 6. Echocardiography

Graphs demonstrating significantly decreased LV chamber area at the papillary level (A) and significantly enhanced LVEF (B) in the NRG-HG group compared to all controls. Measurements were determined by short-axis view on ECHO (* denotes $p<0.05$ for each group vs. NRG-HG).

NIH-PA Author Manuscript
NIH-PA Author Manuscript
NIH-PA Author Manuscript

NIH-PA Author Manuscript
NIH-PA Author Manuscript
NIH-PA Author Manuscript

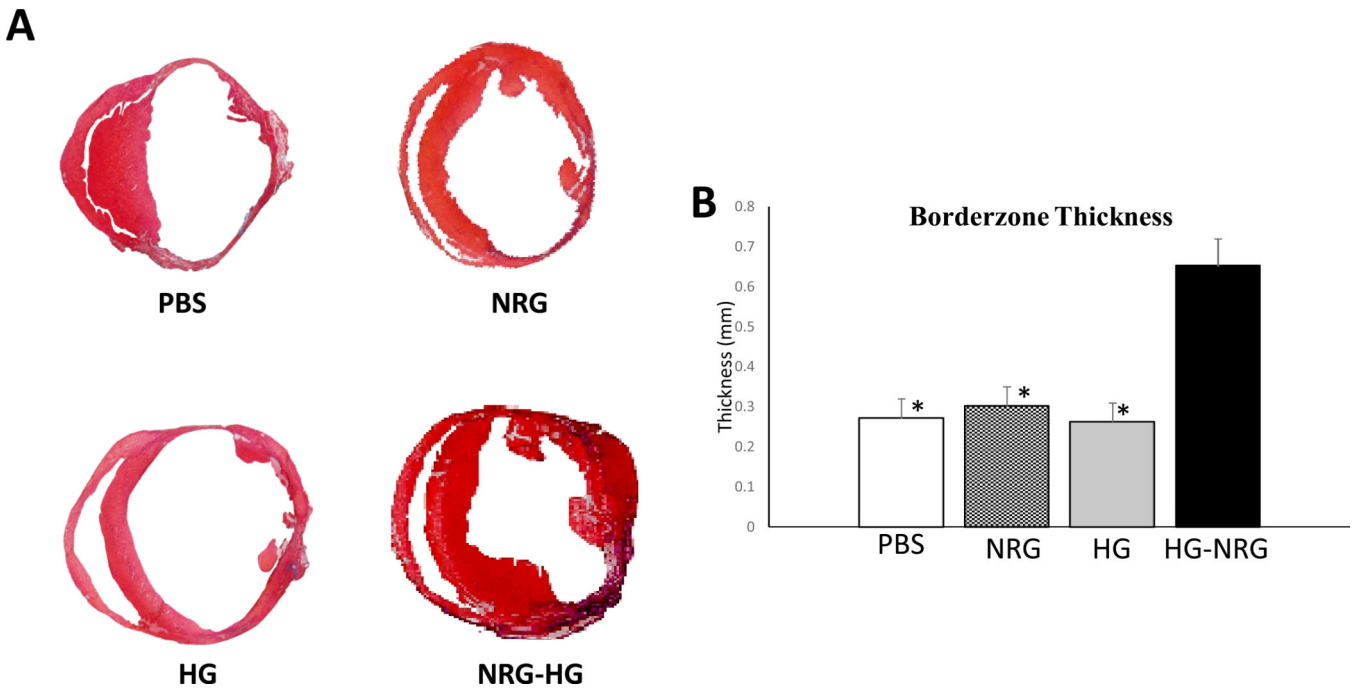

Figure 7. Increased borderzone thickness

Photographs of Masson's Trichrome stained heart sections 14 days following treatment (A). NRG-HG treated animals demonstrated significantly augmented borderzone thickness (* denotes $p<0.01$ for each group vs. NRG-HG) (B).